

VideoOrion: Tokenizing Object Dynamics in Videos

Yicheng Feng^{1,2*} Yijiang Li^{3,2*} Wanpeng Zhang¹ Sipeng Zheng² Zongqing Lu^{1,2†}

¹School of Computer Science, Peking University

²Beijing Academy of Artificial Intelligence

³University of California, San Diego

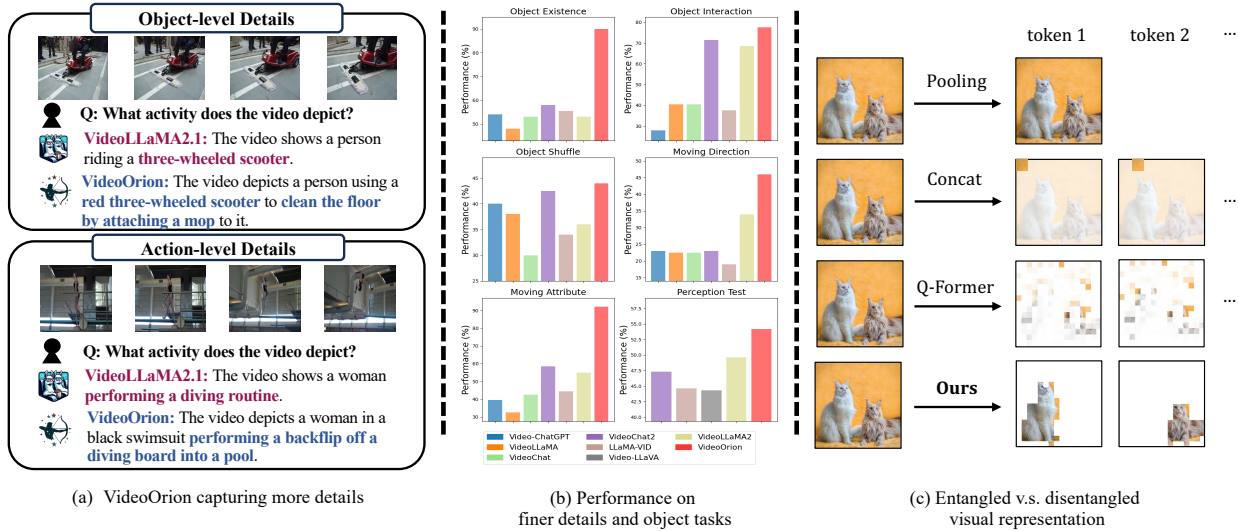


Figure 1. With a set of *object tokens* that explicitly encode semantics about object dynamics, VideoOrion can (a) grasp finer details in videos and (b) perform better in video understanding tasks related to object details from MVBench and Perception-Test. We illustrate previous methods to encode video tokens in (c), including: (1) spatial pooling that pools features of the whole frame into a single token; (2) concatenating adjacent patch tokens into a single token; (3) aggregating patch tokens with query tokens through Q-Former. While these methods can result in semantically entangled representations, our proposed *object tokens* provide disentangled semantics.

Abstract

We present *VideoOrion*, a *Video Large Language Model (Video-LLM)* that explicitly captures the key semantic information in videos—the spatial-temporal dynamics of objects throughout the videos. *VideoOrion* employs expert vision models to extract object dynamics through a detect-segment-track pipeline, encoding them into a set of object tokens by aggregating spatial-temporal object features. Our method addresses the persistent challenge in *Video-LLMs* of efficiently compressing high-dimensional video data into semantic tokens that are comprehensible to LLMs. Compared to prior methods which resort to downsampling the original video or aggregating visual tokens using resam-

plers, leading to information loss and entangled semantics, *VideoOrion* not only offers a more natural and efficient way to derive compact, disentangled semantic representations but also enables explicit object modeling of video content with minimal computational cost. Moreover, the introduced object tokens naturally allow *VideoOrion* to accomplish video-based referring tasks. Experimental results show that *VideoOrion* can learn to make good use of the object tokens, and achieves competitive results on both general video question answering and video-based referring benchmarks.

1. Introduction

The unprecedented performance of Large Language Models (LLMs) [16, 37, 48] has spurred significant interest in ex-

* Equal contribution.

† Correspondence to <zongqing.lu@pku.edu.cn>

tending these models’ capabilities beyond text, which catalyzes the development of multi-modal large language models (MLLMs) [4, 9, 31, 46, 60]. MLLMs aim to process and understand diverse input modalities, thereby enabling them to address a broader spectrum of real-world tasks. MLLMs achieve this by integrating information from various modalities through tokenization and alignment with text tokens. However, a significant challenge lies in efficiently encoding the information from multi-modal inputs into a limited number of tokens, particularly for Video-LLMs, as videos encapsulate much more complex and detailed information than text or other input modalities.

To compress high-dimensional visual information into a more compact representation, existing studies typically employ downsampling or pooling techniques prior to tokenization [23, 34] and utilize various aggregation modules to reduce the number of visual tokens, thereby managing computational costs [1, 14, 26]. However, there are several limitations. First, due to computational constraints, Video-LLMs usually only sample a small fraction of the frames in the video for inference (e.g., sample 8 or 16 frames out of thousands of frames for a video of about 1 minute). Despite being more efficient, they inevitably incur information loss, particularly in the fine-grained dynamics of scenes, objects, and interactions. The discretized frames fail to provide sufficient information for Video-LLMs to model the long-range dynamics within videos. We hypothesize that this limitation is the primary reason why current Video-LLMs can only grasp a general understanding of the video, while their ability to capture finer details remains limited. Furthermore, most existing models encode video tokens by processing image patch tokens through a vision encoder, often neglecting the explicit semantics embedded within these visual tokens. This oversight can result in semantically entangled representations [52]. In contrast, text tokens inherently possess clear and well-defined semantics, creating a significant gap that makes it challenging for the LLM to effectively align the ambiguous visual tokens with the semantically precise text tokens.

In this paper, we present VideoOrion, with a novel method for video tokenization that aggregates video features spatially and temporally based on the objects present in the video, resulting in *object tokens*. This is inspired by the fact that humans always identify the semantics of objects from visual observations before incorporating visual information into thought processes. Just as commonly used tokenizers in text processing, we believe that the tokenizer for the visual modality also needs to provide tokens with richer semantics to enhance the model’s understanding of visual content, while one key aspect of visual semantics lies in the object dynamics. Therefore, we propose to incorporate the object tokens into Video-LLMs. We also supplement the object tokens by a set of *context tokens* pro-

duced by a Video Projector, which provides contextual information beyond the objects in the field of view. Compared to context tokens that provide general information, each object token can distinctly encapsulate fine-grained information regarding a specific object or instance in the video. Moreover, multiple object tokens can better aid the model in comprehending spatial relationships at the object level. Compared with downsampling or global aggregation, our object-centric feature aggregation approach provides semantically more efficient visual tokens (see Figure 1).

To extract object tokens from videos, we propose a detect-segment-track pipeline that leverages several expert models to assist in extracting object semantics. Utilizing knowledge from vision models is more effective in modeling object dynamics into tokens, compared to solely relying on video-text pairs for pretraining. This process incorporates the advanced visual capabilities of expert models into Video-LLMs. Specifically, by following this pipeline, we obtain mask lists of objects changing over time in the video, and then we fuse the objects’ features through mask pooling and temporal pooling, from both spatial and temporal dimensions. The two branches of VideoOrion and its instruct-following capability are trained in three training stages, and we demonstrate its promising video understanding ability through multiple benchmarks. Besides, the object tokens also provide additional support for video-based referring tasks. The main contributions of this paper can be summarized as follows:

- We present a novel Video-LLM, VideoOrion, which features an Object-Centric Branch with the special capability to model object dynamics from input videos through a set of *object tokens*.
- To encode object dynamics from videos into tokens, we propose a detect-segment-track pipeline that leverages knowledge from expert vision models to extract object masks across frames.
- Our experiments show that the proposed Object-Centric Branch brings robust performance improvements, and VideoOrion achieves competitive results on both general video question answering and video-based referring tasks.

2. Related Work

Video-LLMs. Most existing Video-LLMs extend the framework of image-based MLLMs, proposing various adapters to cope with the large number of visual tokens encoded by image-level pretrained visual encoders such as CLIP [43]. Popular models include Video-ChatGPT [34] which uses spatial-temporal pooling; VideoChat [26], VideoChat2 [27] and VideoLLaMA [60] which use Q-Former [25, 63]; MiniGPT4-Video [3] which concatenates adjacent visual tokens and uses linear mapping; VideoLLaMA2 [14] which uses 3D convolution blocks; and

LLaMA-VID [28] which uses cross attention between visual and text embeddings. These efforts have achieved good results, but they fail to focus on the semantics of visual tokens, leaving the parsing of token semantics to LLMs.

There are also studies that pay attention to the semantic aggregation of visual tokens. Chat-univi [22] aggregates visual tokens into dynamic visual tokens with DPC-KNN [15], a clustering algorithm. While this method merges similar visual tokens to reduce redundancy, our approach merges visual tokens in an object-centric manner to ensure clear semantics. Video-LaVIT [23] employs MPEG-4 compression algorithm to extract videos into key frames and motion information and applies VQ-VAE to encode motion tokens. While we also split videos with key frames, we focus on the semantics of objects instead of the general motion. Slot-VLM [52] shares similar idea with ours, leveraging slot attention to cluster object-centric and event-centric concept tokens. Our method differs from theirs in that we employ expert vision models to precisely extract objects, and we perform temporal fusion to encode the dynamics of objects across frames so that our object tokens carry more integrated information about the present objects. Artemis [42] also applies ROI tracking to get target-specific features for visual tokens, but it focuses on video-based referential understanding and only cares about the target object. In contrast, we tend to make Video-LLMs improve the object-centric understanding capabilities and aggregate object tokens for each object identified in the observations.

Visual models for object segmentation. When humans incorporate visual information into reasoning, they naturally segment and extract visual content based on semantics, particularly in identifying distinct objects or entities. Although existing MLLMs often overlook this aspect, this semantic abstraction has numerous corresponding tasks in the field of computer vision, such as object detection [8, 38, 55, 59], instance segmentation [12, 19], video object segmentation [41, 50, 54], and so on. We propose to utilize these expert models to help encode object dynamics, instead of relying on video-text pairs only. In this paper, after various attempts, we apply the combination with GroundingDINO [32] as the object detection model, SAM [24] as the segmentation model, and Xmem [13] as the multi-object tracking model. We believe that these extensive research achievements in computer vision can assist Video-LLMs in better extracting semantics at the visual level.

3. Methodology

3.1. Overall Architecture

We propose VideoOrion, which is characterized by an Object-Centric Branch alongside the Video-Centric Branch for video content tokenization, illustrated in Figure 2. Existing research on Video-LLMs has focused on designing

effective Video-Centric Branches, proposing various architectures such as the spatial-temporal pooling layer [34], Q-former [25, 60], and STC Connector [14]. In contrast, we introduce the Object-Centric Branch, which utilizes expert visual models to extract object dynamics in the video as semantic tokens and connect them to the LLM. The Object-Centric Branch and the Video-Centric Branch operate independently, with the downstream LLM responsible for integrating the semantic information from both branches. Consequently, VideoOrion is adaptable to a variety of architectures for the Video-Centric Branch.

3.2. Video-Centric Branch

Given a video $V_i \in \mathbb{R}^{T \times H \times W \times C}$, where T is the frame number, the Video-Centric Branch employs a Video Projector to convert the high-dimensional video data into a series of tokens, which we call *context tokens*, since they contain general information in the video. VideoOrion allows for various Video Projector designs, and in this paper, we adopt the STC Connector proposed by VideoLLaMA2 [14], as it better preserves spatial and temporal information in the video, enabling the resulting visual tokens to be more effectively associated with our object tokens. Specifically, in this branch, we first sample a fixed number of frames from the video, and use a vision encoder such as CLIP (ViT-L/14) [43] to encode each frame, resulting in the embedding $x_i \in \mathbb{R}^{t_v \times h \times w \times D}$, where t_v is the number of sampled frames, and $h = H/p, w = W/p$ are the resolution of visual embeddings, $p = 14$ for ViT-L/14. Then, we use STC Connector, which is composed of two RegStage blocks [44] and a 3D convolution block, followed by an MLP projector, to transform x_i into context tokens $v_i \in \mathbb{R}^{N_v \times d}$, where N_v is the number of context tokens and d is dimension of the LLM decoder’s token embedding space.

3.3. Object-Centric Branch

In the Object-Centric Branch, we aim to extract a small set of *object tokens* from the whole video, each containing semantic information about the dynamics of an object or instance that appears in the video. The idea here is to aggregate the rich features of the video based on individual objects, thereby obtaining compact features with clear semantics to be used as tokens for the LLM. Therefore, in this branch, we need to achieve the following: 1) Identify various objects present in the video; 2) Track the dynamics of the objects within the video; 3) Aggregate the features of the same object into a single token. Based on this, we first propose a detect-segment-track pipeline that leverages off-the-shelf vision models to obtain the masks of objects. Then we design an architecture called Object Projector to encode the object tokens. Details are illustrated in the following.

Detect-segment-track pipeline. Identifying and tracking objects in videos presents a significant challenge due to

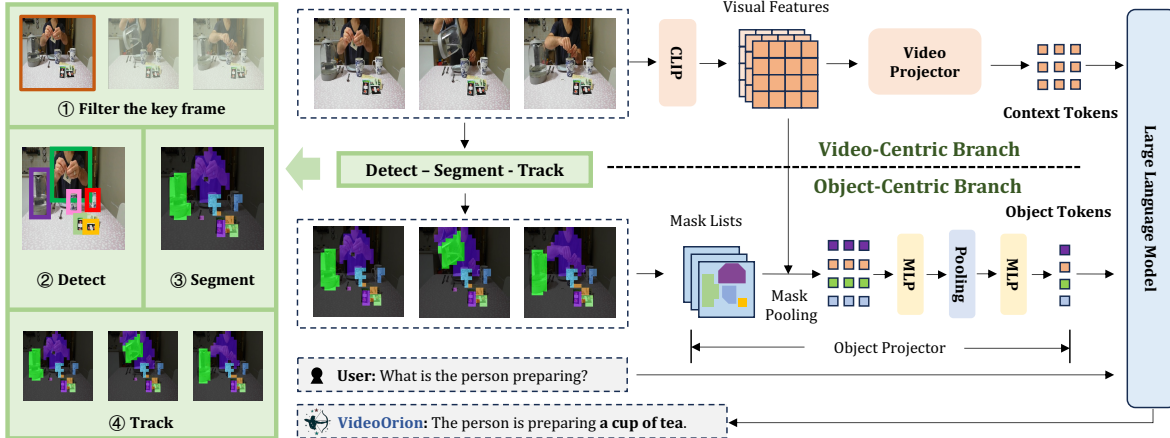


Figure 2. The overall architecture of VideoOrion. Two branches are employed to encode the video content into tokens: the Video-Centric Branch encodes the general information with *context tokens*, while the Object-Centric Branch encodes the dynamics of each object present in the video into an *object token*. Two kinds of tokens are fed together to the LLM, and the LLM is responsible for integrating the semantic information from both branches and generating responses to the text inputs. The detect-segment-track pipeline is used to extract masks of the objects over time.

the dynamic nature of the objects and changes in the scene, which can result in objects leaving or entering the frame over time. Tracking only the objects present in the first frame may lead to a substantial loss of information. One approach is to uniformly sample several frames and segment the video into multiple clips for object identification and tracking. However, this method can cause the same object to be misidentified as different objects across clips and also fail to accurately capture new objects’ appearances. Another method is to employ tracking algorithms that can automatically capture newly appearing objects; however, these algorithms typically only identify close-set objects, making them unsuitable for general videos. Therefore, we propose a new method to segment the video based on the differences in the objects present in the frames.

Specifically, we first sample a certain number of frames from the video, get $\{f_1, f_2, \dots, f_n\}$. For each frame, we use RAM++ [20], an image recognition model, to label it with a series of tags. We then employ NLTK [6], a natural language processing tool, to filter these tags for concrete nouns, while also incorporating synonyms of these nouns, to get a tag set list $\{l_1, l_2, \dots, l_n\}$. These tags allow us to identify the objects present in the frames. Then we set two thresholds θ_a and θ_b . For each frame, we apply θ_a to filter out frames with a low number of tags, as these frames are often noisy: $\mathcal{F}_1 = \{f_u \mid u \in \{1, \dots, n\}, |l_u| > \theta_a\}$. The first frame in \mathcal{F}_1 is designated as the first key frame. Next, for each frame, we use θ_b to assess whether the overlap of its tags with those of the previous key frame falls below this threshold $|l_u \cap l_{key}| < \theta_b$. When the overlap is small, we consider that a significant change in objects has occurred, and we designate this frame as a new key frame. We set the thresholds θ_a and θ_b based on the actual performance

of RAM++, and in our experiments we use $\theta_a = 3$ and $\theta_b = 2$. Following this process, we can obtain a series of key frames that segment the video into different clips based on the appearance of objects.

Given key frames, we apply GroundingDINO [32] with the ‘generic’ mode at the *detect* stage, as it is efficient and performs well, to produce object region proposals for each key frame.¹ Then, at the *segment* stage, we apply SAM [24] to transform these bounding box proposals into masks. At the *track* stage, we first sample t_o frames from the video, and split the sampled frames with the key frames into several clips. Typically t_o can be much greater than t_v , since it is not related to the token numbers and thus would not incur much cost. In our experiments, we use $t_v = 8$, and use $t_o = 64$ for short videos and $t_o = 128$ for videos longer than 1 minute. This brings another benefit that the object tokens can contain more detailed dynamic information compared to context tokens. Then we use Xmem [13], a multi-object tracking algorithm, to track all object masks across the whole video clips start with each key frame, leading to a set of object mask lists $\mathcal{M} = \{M_1, M_2, \dots, M_{N_{oi}}\}$, where N_{oi} is the total number of identified objects in the video V_i , and M_j is the mask list of object j across frames.

Object Projector. The Object Projector translates the object mask lists into object tokens. Each object j that appears in k frames has a list of masks $M_j = \{m_j^{f_{j1}}, m_j^{f_{j2}}, \dots, m_j^{f_{jk}}\}$. We perform mask pooling with each mask to fuse the CLIP features of the corresponding frames f_{j1}, \dots, f_{jk} . Then we use temporal pooling following an MLP projector to fuse the spatially pooled features into

¹We have also tried to use the tags of the key frames as the prompt for GroundingDINO, but there is no better performance.

Table 1. Datasets used in the Object-Centric Branch pretraining stage and the Multi-modal instruction tuning stage.

Training Stage	Data Modality	Object Tokens	Data Source	Dataset Size
Object-Centric Branch pretraining	video-text	✓	InternVid-10M, OpenVid-1M	700K
Multi-modal instruction tuning	video-text	✓	Video-ChatGPT, VideoChat2	1.4M
	image-text	✓	LLaVA	625K
	text-only		Video-LLaVA	40K

a single token. The mask pooling and the temporal pooling operations, from the spatial and temporal dimensions respectively, aggregate video features in an object-centric manner.² Finally, an MLP projector transforms each token into the embedding space of the LLM decoder. For the whole video V_i , we get N_{oi} object tokens $o_j \in \mathbb{R}^d, j \in \{1, \dots, N_{oi}\}$.

3.4. Training and Dataset

In this paper, we present two versions of our framework: VideoOrion, which uses CLIP (ViT-L/14) [43] as the vision encoder and Mistral-Instruct-7B [21] as the LLM backbone; and VideoOrion+, which uses SigLIP (so400m-patch14-384) [58] as the vision encoder and Qwen2-7B [53] as the LLM backbone. To feed context tokens and object tokens together with text tokens to the LLM, we formulate an input template as follows:

User: $\langle v \rangle$ Here is a list of objects and instances in the video: $\langle o_1 \rangle, \langle o_2 \rangle, \dots, \langle o_N \rangle$ $\langle \text{Instruction} \rangle$
Assistant: $\langle \text{Answer} \rangle$

where $\langle v \rangle$ contains the context tokens of the video sample, and $\langle o_1 \rangle, \langle o_2 \rangle, \dots, \langle o_N \rangle$ are the object tokens.

The training procedure is then divided into three stages: 1) Video-Centric Branch pretraining; 2) Object-Centric Branch pretraining; 3) Multi-modal instruction tuning.

Video-Centric Branch pretraining. In this stage, only the Video Projector is optimized with video-text and image-text pairs, without object tokens involved. Thus, we use the pretrained checkpoints of STC-Connector provided by VideoLLaMA2 directly, which are trained on 12.2M vision-language data samples.

Object-Centric Branch pretraining. In this stage, the pretrained Video Projector is frozen and we only optimize the Object Projector with video-text pairs. We construct a dataset here using captioned videos sourced from InternVid-10M [51] and OpenVid-1M [36]. We first filter InternVid-10M using aesthetic scores and UMT-SIM scores, which can indicate the video quality and the video-caption similarity of each data sample respectively, to obtain a subset of size 1.4M. Then we mix this subset with OpenVid-1M and filter the resulting dataset with noun-phrase concept

²The discussion of different architectures of Object Projector can be found in Section 4.5.

balance, following LLaVA [31]. Finally, we get a pretraining dataset with 700K video-text pairs. We preprocess the dataset with the detect-segment-track pipeline to obtain the object mask lists, for training efficiency.

Multi-modal instruction tuning. In the final stage, we only freeze the vision encoder, and optimize the Video Projector, the Object Projector, and the LLM backbone together, with multi-modal instruction tuning datasets. We adopt the training data from Video-LLaVA[29], with 100K video-text, 625K image-text, and 40K text-only instruction-following data samples, and from VideoChat2 [27], with 1.3M video-text instruction-following data samples. We preprocess the video-text samples and image-text samples with the detect-segment-track pipeline to obtain the object mask lists here. For images, we treat them as single-frame videos, and the tracking model is not used in the pipeline.

The training objective of all three stages is the auto-regressive cross-entropy loss. We summarize the datasets used in the Object-Centric Branch pretraining stage and the multi-modal instruction tuning stage in Table 1.

4. Experiments

4.1. Experimental Setup

In our experiments, we sample $t_v = 8$ frames from each video for the Video-Centric Branch for VideoOrion, and set $t_v = 16$ for VideoOrion+. And we sample $t_o = 64$ frames from short videos and $t_o = 128$ frames from videos longer than 1 minute for the Object-Centric Branch. We set $\theta_a = 3$ and $\theta_b = 2$ when extracting key frames to split the video with RAM++, which we find have the best performance, and the number of sampled frames for tagging is set to $n = 16$ for Object-Centric Branch pretraining and $n = 64$ for multi-modal instruction tuning. We resize and crop each frame to 336×336 for CLIP and 384×384 for SigLIP in the Video-Centric Branch, and we only perform resize to frames in the Object-Centric Branch so that the features can align with the masks. The learning rates in our two training stages are set to $1e - 4$ and $5e - 6$, all with a warmup ratio of 0.03. In the Object-Centric Branch pretraining stage, the global batch size is 256, while in the multi-modal instruction tuning stage the global batch size is 128. In all stages, we train for just one epoch. VideoOrion is trained on $8 \times$ A800 GPUs, and VideoOrion+ is trained on $64 \times$ A800 GPUs.

Table 2. The overall performance of our framework compared with the state-of-the-art Video-LLMs. We provide results on four MC-VQA benchmarks and one OE-VQA benchmark. All these models use the 7B-sized LLM backbone except ShareGPT4Video-8B. For the Frame Number column, we refer to the number of frames sampled in the Video-Centric Branch for VideoOrion and VideoOrion+.

Model	Frame Number	MVBench Acc.	Egoschema Acc.	Perception-Test Acc.	Video-MME w/o / w subs	ActivityNet-QA Acc. / Score
LLaMA-VID[28]	1fps	41.9	38.5	44.6	25.9/-	47.4/3.3
TimeChat[45]	-	38.5	33.0	-	-	-
Chat-UniVi[22]	64	-	-	-	40.6/45.9	46.1/3.3
LLaVA-NeXT-Video[62]	32	46.5	43.9	48.8	33.7/-	53.5 /3.2
ShareGPT4Video-8B[10]	16	51.2	-	-	39.9/43.6	-
VideoChat2[27]	16	60.4	54.4	47.3	39.5/43.8	49.1/3.3
Video-LLaVA[29]	8	41.0	38.4	44.3	39.9/41.6	45.3/3.3
VideoLLaMA[60]	8	34.1	-	-	-	12.4/1.1
VideoLLaMA2[14]	8	53.4	50.5	49.6	45.1/46.6	49.9/3.3
VideoOrion	8	58.3	57.6	53.4	46.1/48.0	50.3/3.5
<i>Models with Qwen-2-7B LLM backbone</i>						
LongVA[61]	64	-	-	-	52.4/-	-/2.8
VideoLLaMA2.1[14]	16	57.3	53.1	54.9	54.9/56.4	53.0 /3.4
VideoOrion+	16	64.08	57.2	57.3	55.6 / 57.5	52.4/3.5

4.2. Video Question Answering

Evaluation benchmarks. We comprehensively evaluate the video understanding capabilities of VideoOrion and VideoOrion+ on four multi-choice video question answering (MC-VQA) benchmarks including MVBench [27], EgoSchema [35], Perception-Test [40] and VideoMME [18], which feature videos of varying lengths and types. We report the accuracies for the benchmarks in our results. We also test on an open-ended video question answering (OE-VQA) benchmark ActivityNet-QA [57], where we employ ChatGPT to evaluate the answer generation qualities. Following Maaz et al. [34], we require ChatGPT to output two metrics for each generated answer: a yes/no indicator that signifies whether the predicted answer matches the correct answer, and a score ranging from 0 to 5 that reflects the degree of alignment between the model output and the correct answer, where 5 represents the highest level of matching. We report the proportion of “yes” as the accuracy, as well as the average score.

Zero-shot performance. We compare the overall performance of VideoOrion and VideoOrion+ with the state-of-the-art Video-LLMs in Table 2. VideoOrion achieves competitive performance compared with the baseline models. On EgoSchema, Perception-Test, and VideoMME, VideoOrion obtains the best performance. On MVBench, VideoOrion achieves the second-best performance, slightly lower than VideoChat2 which is trained on the whole instruction-tuning training data of MVBench. On ActivityNet-QA, VideoOrion is the best in terms of score and the second-best in accuracy. Since videos in ActivityNet primarily contain activities of individual humans, the advantages brought by object tokens may not be significantly reflected. VideoOrion consistently outperforms VideoLLaMA2, the model with the same Video-Centric

Branch architecture, by 4.9%, 7.1%, 3.8%, 1/1.4% and 0.4/0.2% on all benchmarks respectively, showing the effectiveness of our proposed Object-Centric Branch for general video understanding.

With the stronger LLM backbone Qwen2, VideoOrion+ gains improved performance, especially on MVBench, Perception-Test, and VideoMME. With the same LLM backbone, VideoOrion+ outperforms VideoLLaMA2.1 by 2.4% in accuracy on average.

4.3. Video-based Referring

With our proposed Object-Centric Branch, VideoOrion can naturally accomplish video-based referring tasks, a capability that common Video-LLMs typically lack. To make VideoOrion perform video-based referring, we simply format the input prompt template as follows:

User: <v> What is <o> doing in this video?
Assistant: <Answer>

where we insert the object token corresponding to the referring target in the video into the instruction. We evaluate the performance on the VideoRef45K benchmark proposed by Artemis[42], which consists of video question-answer samples with box-level prompts indicating the referring target in videos. To encode the object tokens, we use the bounding box prompts provided by VideoRef45K and use SAM to extract masks of the targets.

We train two types of models with a subset of VideoRef45K, which includes data sourced from VID-Sentence [11] (8K), HC-STVG [47] (10K) and LaSOT [17] (8K). For the first model VideoOrion-Ref, we integrate the data into the multi-modal instruction tuning stage with instruction following data provided by VideoLLaVA to train VideoOrion, and we test its zero-shot capability.

For the second type, we present VideoOrion-Ref-FT and VideoOrion-Ref-FT+, where we finetune VideoOrion and VideoOrion+ with the referring data for 3 epochs, following the training procedure of Artemis. We evaluate the models with metrics including BLEU@4 [39], METEOR [5], ROUGE_L [30], CIDEr [49] and SPICE [2]. We compare the results with Artemis, a video-based referring model, and Merlin [56], a multi-frame-based referring model, in Table 3.

Table 3. Performance on the video-based referring task proposed by Qiu et al. [42].

Model	BLEU@4	METEOR	ROUGE_L	CIDEr	SPICE
Merlin[56]	3.3	11.3	26.0	10.5	20.1
Artemis[42]	15.5	18.0	40.8	53.2	25.4
VideoOrion-Ref	17.5	19.5	43.0	69.7	28.4
VideoOrion-Ref-FT	19.0	21.0	43.8	79.6	30.4
VideoOrion-Ref-FT+	19.7	21.5	45.4	90.6	31.4

We can see that all our models outperform the baselines on all evaluation metrics. Notably, VideoOrion-Ref shows good zero-shot performance, with a small amount of referring data involved in the instruction tuning stage. Moreover, following the same training procedure as Artemis with the finetuning stage, VideoOrion-Ref-FT and VideoOrion-Ref-FT+ achieve significantly better results. This demonstrates that the object tokens convey accurate object semantics so that the model can clearly capture the features of targets. Furthermore, our model provides an approach that enables Video-LLMs to possess both general video understanding and video-based referring capabilities.

4.4. Ablation Study

Effect of the object tokens. We first study the improvement brought by our proposed Object-Centric Branch by training a baseline model with only the Video-Centric Branch. For a fair comparison, in this experiment, we train VideoOrion in all three stages, with pretraining data including 702K video-text pairs provided by Valley [33] and 558K image-text pairs provided by LLaVA [31] for the Video-Centric Branch pretraining stage. We use our filtered 700K data samples in the second stage, and use instruction following data provided by Video-LLaVA [29] in the last stage. For the baseline model, we use the pretraining data in the first two stages together (1.4M video-text pairs and 558K image-text pairs) for Video-Centric Branch pretraining, and use the same instruction tuning data.

The comparison of results in Table 4 shows how our Object-Centric Branch improves the overall video understanding capabilities. VideoOrion with object tokens involved consistently outperforms the ablative baseline. It shows that, trained on the same data, VideoOrion can better grasp the content of the videos with the introduction of the object tokens, which models object dynamics. Although

Table 4. Ablation study on the Object-Centric Branch. We compare the performance of VideoOrion with a baseline VideoLLaMA2. For a fair comparison, VideoLLaMA2 is trained with the same amount of pretrain data as VideoOrion.

Model	MVBench	Egoschema	Perception	VideoMME	ActNet
(baseline)	41.9	41.3	43.6	44.1	43.0
VideoOrion	44.2	44.5	46.3	46.1	43.3

the number of object tokens is relatively small, the impact is obvious.

Effect of the Object-Centric Branch pretraining stage.

Then we evaluate the effect of the Object-Centric Branch pretraining stage. In Table 5, we show a baseline that the Object Projector is not pretrained and is only optimized in the multi-modal instruction tuning stage. For time efficiency, in this experiment, we sample 100K from 1.3M instruction following data from VideoChat2 in the instruction tuning stage. We find that the baseline achieves a performance drop in most benchmarks, demonstrating that the object tokens, like normal visual tokens, also need to be pretrained to align with text, so the pretraining stage is necessary.

Table 5. Ablation study on the Object-Centric Branch pretraining stage.

Object Pretrain	MVBench	Egoschema	Perception	VideoMME	ActNet
✗	51.2	43.5	50.5	46.8	44.3
✓	52.5	51.3	49.7	47.6	46.3

4.5. Architecture of the Object Projector

Here we explore the influence of different architectures used for the Object Projector. Given the features of objects after mask pooling across frames, we conduct experiments with different methods to encode the features into object tokens: 1) **MLP** is exactly the method used by VideoOrion in this paper, which employs an MLP to transform the object features, followed by average pooling in the temporal dimension; 2) **Attention** layer encodes the features of the same object across frames with a Transformer Encoder layer, followed by average pooling in the temporal dimension; 3) **Linear** layer uses a linear transformation followed by average pooling in the temporal dimension; 4) **Pooling** employs temporal average pooling directly to the object features; 5) **LSTM** layer uses a 2-layer LSTM network to encode the object features. The results are shown in Table 6.

From the results, while the performances are robust across different architectures, we find that our architecture using only MLP performs best, compared with more advanced structures like the Transformer encoder. This may indicate that projectors only need a simple structure to achieve feature alignment, whereas a relatively complex

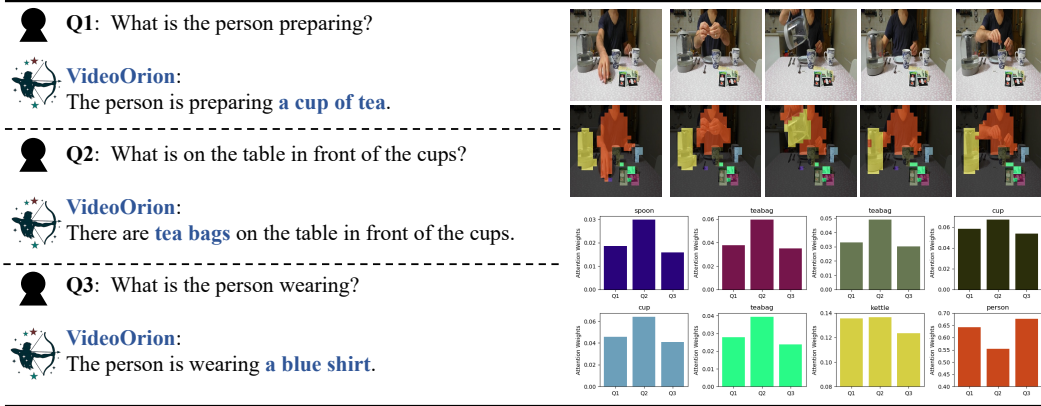


Figure 3. The case study shows how VideoOrion makes use of the object tokens with different instructions. Top-right corner shows the example frames and the object masks of the input video. On the left are three different questions, and the responses provided by VideoOrion. We plot the normalized attention weights of all object tokens on the bottom-right corner, where each bar chart presents the different attention weights of the same object token given the three input questions, with the title indicating the object that corresponds to the object token. The color of the bars indicates the corresponding object mask in the shown frames.

Table 6. Performance of VideoOrion with different Object Projectors. We explore mlp (default), attention, linear, lstm layers and plain average pooling.

Architecture	MVBench	Egoschema	Perception	VideoMME	ActNet	Avg.
mlp (ours)	48.0	51.5	46.9	45.6	41.6	46.73
attention	48.8	45.9	47.6	44.3	41.0	45.51
linear	47.3	47.2	46.1	44.1	42.9	45.52
avg pooling	47.3	47.5	46.0	45.4	41.9	45.61
lstm	49.5	47.0	47.8	45.1	42.9	46.45

architecture may have a negative impact.

4.6. Case Study

In this section, we show how VideoOrion makes use of the object tokens through a case study. With an input video shown in Figure 3, we ask VideoOrion three different questions, and we visualize the change in the attention weights of all the object tokens from the last decoder layer of the LLM backbone of VideoOrion. We normalize the attention weights so that the attention weights of all eight object tokens are sum to 1. We also visualize the object masks extracted by the detect-segment-track pipeline.

From the charts, we can find that the attention given to the object tokens changes with different input questions, and the more relevant the object is to the question, the higher the attention weight is given to the corresponding object token. For example, for the object token corresponding to the *person* (the last chart), it receives the lowest attention with *Q2*, since the question is not relevant to the person. For *Q1*, the attention gets higher, since the question mentions *person*. However, the attention given to the *person* token is highest with *Q3*, since this question focuses only on the feature of the person in the video. On the other hand, the attention weights given to tokens corresponding to the teabags and cups increase significantly with *Q2*, which can

directly lead to the answer of the question.

From another perspective, for *Q1* which cares about the general content of the video, the attention weights obtained by all object tokens are in the middle among the three questions. For the other two questions, which care about some details, the attention weights become more concentrated on the relevant objects. These phenomena indicate that VideoOrion has learned to better utilize the information provided by object tokens to answer questions, which also demonstrates that our object tokens can effectively enhance the model’s video comprehension capabilities.

5. Conclusion

We propose VideoOrion in this paper, a novel Video-LLM framework, which employs a Video-Centric Branch and an Object-Centric Branch for video content tokenization. Particularly, the Object-Centric Branch extracts object tokens through a detect-segment-track pipeline, with the knowledge from expert vision models, providing more semantically meaningful tokens regarding object dynamics to the LLM backbone. Our experimental results across multiple benchmarks demonstrate the capability of VideoOrion for both general video understanding and video-based referring. Meanwhile, we believe the proposed framework may also be applied to other Video-Centric Branches to introduce referring abilities and understanding for finer details.

Limitations

Our current method also has some limitations. For instance, the detect-segment-track pipeline requires collaboration among multiple vision models, which may introduce additional cost, and can lead to inaccurate mask extraction for videos with low quality. This may be alleviated with

stronger vision models in the future, and we will investigate improvements in the object token encoding process. Besides, the current framework still requires the Video-Centric Branch for context information, and the alignment between the two branches has not been fully studied.

References

- [1] Jean-Baptiste Alayrac, Jeff Donahue, Pauline Luc, Antoine Miech, Iain Barr, Yana Hasson, Karel Lenc, Arthur Mensch, Katherine Millican, Malcolm Reynolds, et al. Flamingo: a visual language model for few-shot learning. In *NeurIPS*, 2022. 2
- [2] Peter Anderson, Basura Fernando, Mark Johnson, and Stephen Gould. Spice: Semantic propositional image caption evaluation. In *ECCV*, 2016. 7
- [3] Kirolos Ataallah, Xiaoqian Shen, Eslam Abdelrahman, Essam Sleiman, Deyao Zhu, Jian Ding, and Mohamed Elhoseiny. Minigt4-video: Advancing multimodal llms for video understanding with interleaved visual-textual tokens. *arXiv preprint arXiv:2404.03413*, 2024. 2
- [4] Jinze Bai, Shuai Bai, Shusheng Yang, Shijie Wang, Sinan Tan, Peng Wang, Junyang Lin, Chang Zhou, and Jingren Zhou. Qwen-vl: A frontier large vision-language model with versatile abilities. *arXiv preprint arXiv:2308.12966*, 2023. 2
- [5] Satantjeet Banerjee and Alon Lavie. Meteor: An automatic metric for mt evaluation with improved correlation with human judgments. In *Proceedings of the acl workshop on intrinsic and extrinsic evaluation measures for machine translation and/or summarization*, 2005. 7
- [6] Steven Bird, Ewan Klein, and Edward Loper. *Natural language processing with Python: analyzing text with the natural language toolkit*. " O'Reilly Media, Inc.", 2009. 4
- [7] Mu Cai, Reuben Tan, Jianrui Zhang, Bocheng Zou, Kai Zhang, Feng Yao, Fangrui Zhu, Jing Gu, Yiwu Zhong, Yuzhang Shang, Yao Dou, Jaden Park, Jianfeng Gao, Yong Jae Lee, and Jianwei Yang. Temporalbench: Towards fine-grained temporal understanding for multimodal video models. *arXiv preprint arXiv:2410.10818*, 2024. 11
- [8] Nicolas Carion, Francisco Massa, Gabriel Synnaeve, Nicolas Usunier, Alexander Kirillov, and Sergey Zagoruyko. End-to-end object detection with transformers. In *ECCV*, 2020. 3
- [9] Jun Chen, Deyao Zhu, Xiaoqian Shen, Xiang Li, Zechun Liu, Pengchuan Zhang, Raghuraman Krishnamoorthi, Vikas Chandra, Yunyang Xiong, and Mohamed Elhoseiny. Minigt-v2: large language model as a unified interface for vision-language multi-task learning. *arXiv preprint arXiv:2310.09478*, 2023. 2
- [10] Lin Chen, Xilin Wei, Jinsong Li, Xiaoyi Dong, Pan Zhang, Yuhang Zang, Zehui Chen, Haodong Duan, Bin Lin, Zhenyu Tang, et al. Sharegpt4video: Improving video understanding and generation with better captions. *arXiv preprint arXiv:2406.04325*, 2024. 6
- [11] Zhenfang Chen, Lin Ma, Wenhan Luo, and Kwan-Yee K Wong. Weakly-supervised spatio-temporally grounding natural sentence in video. *arXiv preprint arXiv:1906.02549*, 2019. 6
- [12] Bowen Cheng, Ishan Misra, Alexander G Schwing, Alexander Kirillov, and Rohit Girdhar. Masked-attention mask transformer for universal image segmentation. In *CVPR*, pages 1290–1299, 2022. 3
- [13] Ho Kei Cheng and Alexander G. Schwing. Xmem: Long-term video object segmentation with an atkinson-shiffrin memory model. In *ECCV*, 2022. 3, 4
- [14] Zesen Cheng, Sicong Leng, Hang Zhang, Yifei Xin, Xin Li, Guanzheng Chen, Yongxin Zhu, Wenqi Zhang, Ziyang Luo, Deli Zhao, et al. Videollama 2: Advancing spatial-temporal modeling and audio understanding in video-llms. *arXiv preprint arXiv:2406.07476*, 2024. 2, 3, 6
- [15] Mingjing Du, Shifei Ding, and Hongjie Jia. Study on density peaks clustering based on k-nearest neighbors and principal component analysis. *Knowl. Based Syst.*, 2016. 3
- [16] Abhimanyu Dubey, Abhinav Jauhri, Abhinav Pandey, Abhishek Kadian, Ahmad Al-Dahle, Aiesha Letman, Akhil Mathur, Alan Schelten, Amy Yang, Angela Fan, et al. The llama 3 herd of models. *arXiv preprint arXiv:2407.21783*, 2024. 1
- [17] Heng Fan, Liting Lin, Fan Yang, Peng Chu, Ge Deng, Sijia Yu, Hexin Bai, Yong Xu, Chunyuan Liao, and Haibin Ling. Lasot: A high-quality benchmark for large-scale single object tracking. In *CVPR*, 2019. 6
- [18] Chaoyou Fu, Yuhan Dai, Yondong Luo, Lei Li, Shuhuai Ren, Renrui Zhang, Zihan Wang, Chenyu Zhou, Yunhang Shen, Mengdan Zhang, et al. Video-mme: The first-ever comprehensive evaluation benchmark of multi-modal llms in video analysis. *arXiv preprint arXiv:2405.21075*, 2024. 6
- [19] Kaiming He, Georgija Gkioxari, Piotr Dollár, and Ross Girshick. Mask r-cnn. In *ICCV*, 2017. 3
- [20] Xinyu Huang, Yi-Jie Huang, Youcai Zhang, Weiwei Tian, Rui Feng, Yuejie Zhang, Yanchun Xie, Yaqian Li, and Lei Zhang. Open-set image tagging with multi-grained text supervision. *arXiv e-prints*, 2023. 4
- [21] Albert Q Jiang, Alexandre Sablayrolles, Arthur Mensch, Chris Bamford, Devendra Singh Chaplot, Diego de las Casas, Florian Bressand, Gianna Lengyel, Guillaume Lample, Lucile Saulnier, et al. Mistral 7b. *arXiv preprint arXiv:2310.06825*, 2023. 5
- [22] Peng Jin, Ryuichi Takanobu, Wancai Zhang, Xiaochun Cao, and Li Yuan. Chat-univi: Unified visual representation empowers large language models with image and video understanding. In *CVPR*, 2024. 3, 6
- [23] Yang Jin, Zhicheng Sun, Kun Xu, Kun Xu, Liwei Chen, Hao Jiang, Quzhe Huang, Chengru Song, Yuliang Liu, Di Zhang, Yang Song, Kun Gai, and Yadong Mu. Video-lavit: Unified video-language pre-training with decoupled visual-motional tokenization. In *ICML*, 2024. 2, 3
- [24] Alexander Kirillov, Eric Mintun, Nikhila Ravi, Hanzi Mao, Chloé Rolland, Laura Gustafson, Tete Xiao, Spencer Whitehead, Alexander C. Berg, Wan-Yen Lo, Piotr Dollár, and Ross B. Girshick. Segment anything. In *ICCV*, 2023. 3, 4
- [25] Junnan Li, Dongxu Li, Silvio Savarese, and Steven C. H. Hoi. BLIP-2: bootstrapping language-image pre-training with frozen image encoders and large language models. In *ICML*, 2023. 2, 3

- [26] KunChang Li, Yinan He, Yi Wang, Yizhuo Li, Wenhai Wang, Ping Luo, Yali Wang, Limin Wang, and Yu Qiao. Videochat: Chat-centric video understanding. *arXiv preprint arXiv:2305.06355*, 2023. 2
- [27] Kunchang Li, Yali Wang, Yinan He, Yizhuo Li, Yi Wang, Yi Liu, Zun Wang, Jilan Xu, Guo Chen, Ping Luo, et al. Mvbench: A comprehensive multi-modal video understanding benchmark. In *CVPR*, 2024. 2, 5, 6
- [28] Yanwei Li, Chengyao Wang, and Jiaya Jia. Llama-vid: An image is worth 2 tokens in large language models. *arXiv preprint arXiv:2311.17043*, 2023. 3, 6
- [29] Bin Lin, Bin Zhu, Yang Ye, Munan Ning, Peng Jin, and Li Yuan. Video-llava: Learning united visual representation by alignment before projection. *arXiv preprint arXiv:2311.10122*, 2023. 5, 6, 7
- [30] Chin-Yew Lin. Rouge: A package for automatic evaluation of summaries. In *Text summarization branches out*, 2004. 7
- [31] Haotian Liu, Chunyuan Li, Qingyang Wu, and Yong Jae Lee. Visual instruction tuning. In *NeurIPS*, 2023. 2, 5, 7
- [32] Shilong Liu, Zhaoyang Zeng, Tianhe Ren, Feng Li, Hao Zhang, Jie Yang, Chunyuan Li, Jianwei Yang, Hang Su, Jun Zhu, et al. Grounding dino: Marrying dino with grounded pre-training for open-set object detection. *arXiv preprint arXiv:2303.05499*, 2023. 3, 4
- [33] Ruipu Luo, Ziwang Zhao, Min Yang, Junwei Dong, Da Li, Pengcheng Lu, Tao Wang, Linmei Hu, Minghui Qiu, and Zhongyu Wei. Valley: Video assistant with large language model enhanced ability. *arXiv preprint arXiv:2306.07207*, 2023. 7
- [34] Muhammad Maaz, Hanoona Abdul Rasheed, Salman Khan, and Fahad Khan. Video-chatgpt: Towards detailed video understanding via large vision and language models. In *ACL*, 2024. 2, 3, 6
- [35] Karttikeya Mangalam, Raiymbek Akshulakov, and Jitendra Malik. Egoschema: A diagnostic benchmark for very long-form video language understanding. In *NeurIPS*, 2023. 6
- [36] Kepan Nan, Rui Xie, Penghao Zhou, Tiehan Fan, Zhenheng Yang, Zhijie Chen, Xiang Li, Jian Yang, and Ying Tai. Openvid-1m: A large-scale high-quality dataset for text-to-video generation. *arXiv preprint arXiv:2407.02371*, 2024. 5
- [37] OpenAI. Gpt-4 technical report. *arXiv preprint arXiv:2303.08774*, 2023. 1
- [38] Maxime Oquab, Timothée Darcet, Théo Moutakanni, Huy Vo, Marc Szafraniec, Vasil Khalidov, Pierre Fernandez, Daniel Haziza, Francisco Massa, Alaaeldin El-Nouby, et al. Dinov2: Learning robust visual features without supervision. *arXiv preprint arXiv:2304.07193*, 2023. 3
- [39] Kishore Papineni, Salim Roukos, Todd Ward, and Wei-Jing Zhu. Bleu: a method for automatic evaluation of machine translation. In *ACL*, 2002. 7
- [40] Viorica Patraucean, Lucas Smaira, Ankush Gupta, Adrià Recasens, Larisa Markeeva, Dylan Banarse, Skanda Koppula, Joseph Heyward, Mateusz Malinowski, Yi Yang, Carl Doersch, Tatiana Matejovicova, Yury Sulsky, Antoine Miech, Alexandre Fréchet, Hanna Klimczak, Raphael Koster, Junlin Zhang, Stephanie Winkler, Yusuf Aytar, Simon Osindero, Dima Damen, Andrew Zisserman, and João Carreira. Perception test: A diagnostic benchmark for multimodal video models. In *NeurIPS*, 2023. 6
- [41] Federico Perazzi, Anna Khoreva, Rodrigo Benenson, Bernt Schiele, and Alexander Sorkine-Hornung. Learning video object segmentation from static images. In *CVPR*, 2017. 3
- [42] Jihao Qiu, Yuan Zhang, Xi Tang, Lingxi Xie, Tianren Ma, Pengyu Yan, David Doermann, Qixiang Ye, and Yunjie Tian. Artemis: Towards referential understanding in complex videos. *arXiv preprint arXiv:2406.00258*, 2024. 3, 6, 7
- [43] Alec Radford, Jong Wook Kim, Chris Hallacy, Aditya Ramesh, Gabriel Goh, Sandhini Agarwal, Girish Sastry, Amanda Askell, Pamela Mishkin, Jack Clark, Gretchen Krueger, and Ilya Sutskever. Learning transferable visual models from natural language supervision. In *ICML*, 2021. 2, 3, 5
- [44] Ilija Radosavovic, Raj Prateek Kosaraju, Ross B. Girshick, Kaiming He, and Piotr Dollár. Designing network design spaces. In *CVPR*, 2020. 3
- [45] Shuhuai Ren, Linli Yao, Shicheng Li, Xu Sun, and Lu Hou. Timechat: A time-sensitive multimodal large language model for long video understanding. In *Proceedings of the IEEE/CVF Conference on Computer Vision and Pattern Recognition*, 2024. 6
- [46] Fangxun Shu, Lei Zhang, Hao Jiang, and Cihang Xie. Audio-visual llm for video understanding. *arXiv preprint arXiv:2312.06720*, 2023. 2
- [47] Zongheng Tang, Yue Liao, Si Liu, Guanbin Li, Xiaojie Jin, Hongxu Jiang, Qian Yu, and Dong Xu. Human-centric spatio-temporal video grounding with visual transformers. *IEEE Transactions on Circuits and Systems for Video Technology*, 2021. 6
- [48] Gemini Team, Rohan Anil, Sebastian Borgeaud, Yonghui Wu, Jean-Baptiste Alayrac, Jiahui Yu, Radu Soricut, Johan Schalkwyk, Andrew M Dai, Anja Hauth, et al. Gemini: a family of highly capable multimodal models. *arXiv preprint arXiv:2312.11805*, 2023. 1
- [49] Ramakrishna Vedantam, C Lawrence Zitnick, and Devi Parikh. Cider: Consensus-based image description evaluation. In *Proceedings of the IEEE conference on computer vision and pattern recognition*, 2015. 7
- [50] Qiang Wang, Li Zhang, Luca Bertinetto, Weiming Hu, and Philip HS Torr. Fast online object tracking and segmentation: A unifying approach. In *CVPR*, 2019. 3
- [51] Yi Wang, Yinan He, Yizhuo Li, Kunchang Li, Jiashuo Yu, Xin Ma, Xinhao Li, Guo Chen, Xinyuan Chen, Yaohui Wang, et al. Internvid: A large-scale video-text dataset for multimodal understanding and generation. In *ICLR*, 2023. 5
- [52] Jiaqi Xu, Cuiling Lan, Wenxuan Xie, Xuejin Chen, and Yan Lu. Slot-vlm: Slowfast slots for video-language modeling. *arXiv preprint arXiv:2402.13088*, 2024. 2, 3
- [53] An Yang, Baosong Yang, Binyuan Hui, Bo Zheng, Bowen Yu, Chang Zhou, Chengpeng Li, Chengyuan Li, Dayiheng Liu, Fei Huang, et al. Qwen2 technical report. *arXiv preprint arXiv:2407.10671*, 2024. 5

- [54] Zongxin Yang, Yunchao Wei, and Yi Yang. Associating objects with transformers for video object segmentation. In *NeurIPS*, 2021. 3
- [55] Lewei Yao, Jianhua Han, Youpeng Wen, Xiaodan Liang, Dan Xu, Wei Zhang, Zhenguo Li, Chunjing Xu, and Hang Xu. Detclip: Dictionary-enriched visual-concept paralleled pre-training for open-world detection. In *NeurIPS*, 2022. 3
- [56] En Yu, Liang Zhao, Yana Wei, Jinrong Yang, Dongming Wu, Lingyu Kong, Haoran Wei, Tiancai Wang, Zheng Ge, Xiangyu Zhang, et al. Merlin: Empowering multimodal llms with foresight minds. In *ECCV*, 2025. 7
- [57] Zhou Yu, Dejing Xu, Jun Yu, Ting Yu, Zhou Zhao, Yueting Zhuang, and Dacheng Tao. Activitynet-qa: A dataset for understanding complex web videos via question answering. In *AAAI*, 2019. 6
- [58] Xiaohua Zhai, Basil Mustafa, Alexander Kolesnikov, and Lucas Beyer. Sigmoid loss for language image pre-training. In *ICCV*, 2023. 5
- [59] Hao Zhang, Feng Li, Shilong Liu, Lei Zhang, Hang Su, Jun Zhu, Lionel M. Ni, and Heung-Yeung Shum. DINO: DETR with improved denoising anchor boxes for end-to-end object detection. In *ICLR*, 2023. 3
- [60] Hang Zhang, Xin Li, and Lidong Bing. Video-llama: An instruction-tuned audio-visual language model for video understanding. In *EMNLP*, 2023. 2, 3, 6
- [61] Peiyuan Zhang, Kaichen Zhang, Bo Li, Guangtao Zeng, Jingkang Yang, Yuanhan Zhang, Ziyue Wang, Haoran Tan, Chunyuan Li, and Ziwei Liu. Long context transfer from language to vision. *arXiv preprint arXiv:2406.16852*, 2024. 6
- [62] Yuanhan Zhang, Bo Li, haotian Liu, Yong jae Lee, Liangke Gui, Di Fu, Jiashi Feng, Ziwei Liu, and Chunyuan Li. Llava-next: A strong zero-shot video understanding model, 2024. 6
- [63] Deyao Zhu, Jun Chen, Xiaoqian Shen, Xiang Li, and Mohamed Elhoseiny. Minigt-4: Enhancing vision-language understanding with advanced large language models. In *ICLR*, 2024. 2

A. Hyperparameters

As illustrated in Table 8, we report additional detailed hyperparameters for VideoOrion and VideoOrion+ used in different training stages.

B. More Examples of the Detect-Segment-Track Pipeline

We show additional examples of the object mask lists extracted through the detect-segment-track pipeline in Figure 4. To provide a clearer illustration of the mask pooling mechanism in our model, we resize the masks and map them to the patch level. As can be seen in most instances, the pipeline effectively identifies the salient objects present in videos, ensuring that the resulting object tokens are enriched with clear and meaningful semantics.

C. More Qualitative Results

Additional qualitative examples of VideoOrion+, VideoOrion-Ref and VideoOrion-Ref-FT+ are presented in Figure 5. These examples highlight our model’s capabilities of capturing interaction details and object dynamics, as well as its enhanced video-based referring capabilities after being trained on this task.

D. Temporal-Understanding Benchmark

In Table 7, we compare VideoOrion and VideoOrion+ against the baseline models VideoLLaMA2 and VideoLLaMA2.1 on short video QA tasks from TemporalBench[7], a benchmark designed to evaluate fine-grained temporal understanding capabilities. The results demonstrate that our models outperform the baselines, highlighting VideoOrion’s superior ability to capture fine-grained temporal details from videos. Intuitively, using Object Projector with the attention or LSTM architecture would be more favorable for understanding temporal information, which we plan to explore further in future research.

Table 7. Results of zero-shot performance on TemporalBench.

Model	Multi-Binary Accuracy (Acc.)	Binary Accuracy (Acc.)
VideoLLaMA2	15.9	57.4
VideoOrion	18.2	59.0
VideoLLaMA2.1	17.9	59.5
VideoOrion+	20.7	60.4

E. Data Scaling

In this section, we demonstrate how our model can benefit from data scaling. To evaluate this, we randomly divide

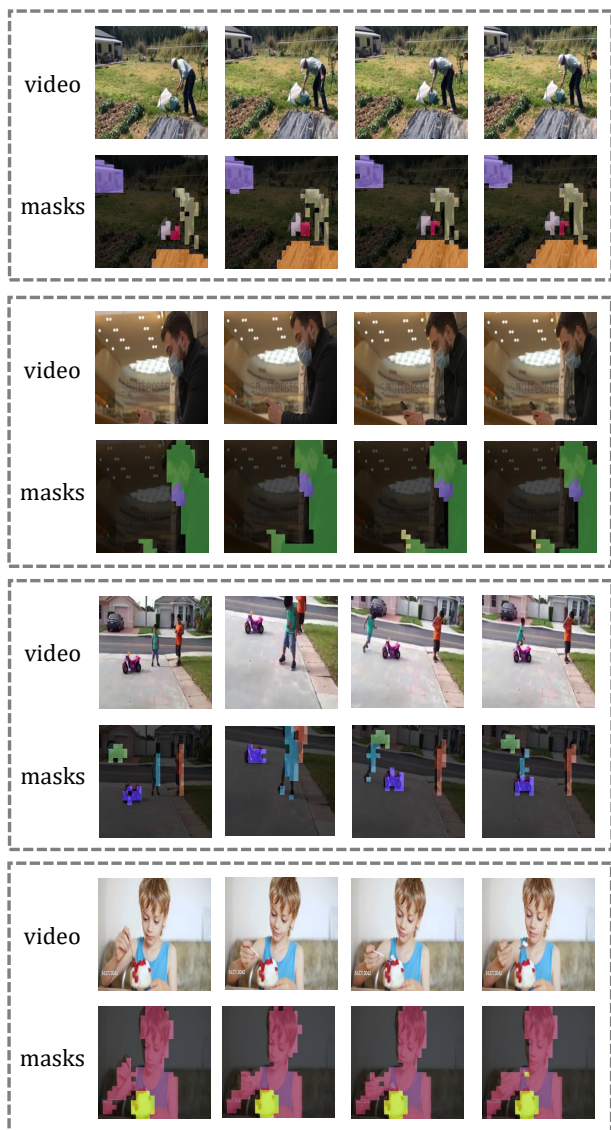


Figure 4. Examples of the detect-segment-track pipeline.

the instruction tuning dataset from VideoChat2 into three parts, and we begin by fine-tuning VideoOrion using only the Video-LLaVA dataset. Subsequently, we progressively incorporate each of the three parts from VideoChat2 into the training data and demonstrate how performance evolve with scaling of the dataset. As per Figure 6, the performances of VideoOrion consistently improve across all four benchmarks, i.e. MVBench, Perception-Test, Video-MME and ActivityNet-QA, with more training data. These results demonstrate VideoOrion’s capacity to effectively harness larger datasets, enabling consistent improvements in performance.

Interaction Details



Q: What unexpected action did the pedestrian take in response to being sprayed with water?

VideoLLaMA2.1: The pedestrian unexpectedly retaliated by **punching the driver in the face** after being sprayed with water.

VideoOrion+: The pedestrian suddenly **grabbed the car door and pulled it open**.

Object Dynamics



Q: Are there any stationary cubes?

VideoLLaMA2.1: Yes, there are cubes that remain stationary in the video.

VideoOrion+: No, the cubes are **not stationary**. They **move around with the cylinder and sphere**.

Video-based Referring



Q: What is **<object>** doing in this video?

VideoOrion-Ref: The woman in **yellow clothes** raises her hand and **touches her hair**, then puts her hand down.

Video-based Referring



Q: What is **<object>** doing in this video?

VideoOrion-Ref-FT+: The woman in **white clothes** **pours water on the man's head**, then **covers her mouth with both hands**.

Figure 5. Qualitative examples of VideoOrion+, VideoOrion-Ref and VideoOrion-Ref-FT+.

Table 8. Training hyperparameters for VideoOrion and VideoOrion+.

Config	VideoOrion			VideoOrion+		
	Stage1	Stage2	Stage3	Stage1	Stage2	Stage3
Vision Encoder	CLIP(ViT-L/14)			SigLIP(so400m-patch14-384)		
LLM Backbone	Mistral-Instruct-7B			Qwen2-7B		
Frame Number	8	8	8	16	16	16
Input Resolution	336	336	336	384	384	384
Learning Rate	$1e-3$	$1e-4$	$5e-6$	$1e-3$	$1e-4$	$5e-6$
Weight Decay	0	0	0	0	0	0
Warmup Ratio	0.03	0.03	0.03	0.03	0.03	0.03
Learning Rate Schedule	cosine	cosine	cosine	cosine	cosine	cosine
Numerical Precision	bfloat16	bfloat16	bfloat16	bfloat16	bfloat16	bfloat16
Batch Size	256	256	128	256	256	128
LLM Sequence Length	2048	2048	2048	2048	2048	2048
Epoch Number	1	1	1	1	1	1
Max Object Token Number	-	-	64	-	-	64

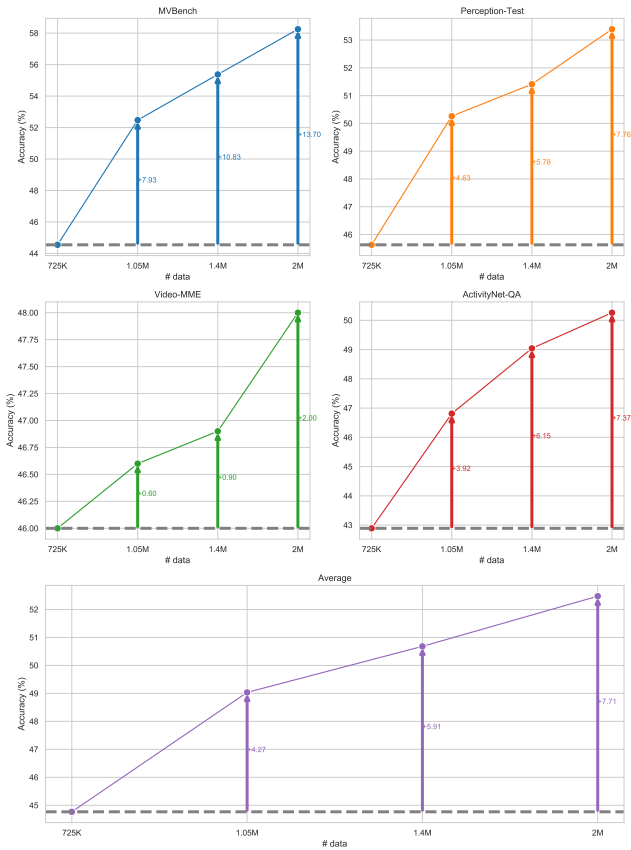


Figure 6. An illustration showcasing how VideoOrion benefits from increased training data.